

Y.C. KIM*, S.S. KIM*, J.U. CHO*[‡]

EXPERIMENTAL STUDY ON FRACTURE PROPERTY OF TAPERED DOUBLE CANTILEVER BEAM SPECIMEN WITH ALUMINUM FOAM

DOŚWIADCZALNE BADANIE PĘKANIA MIMOŚRODOWO ROZCIĄGANIEJ ZWĘŻANEJ PRÓBKII Z BOCZNYM KARBEM WYKONANEJ Z PIANY ALUMINIOWEJ

It is indispensable to evaluate fracture energy as the bonding strength of adhesive at composite material with aluminum foam. This specimen is designed with tapered double cantilever beam by British standards (BS 7991 and ISO 11343). 4 kinds of specimens due to m values of 2, 2.5, 3 and 3.5 are manufactured and compared each other with the experimental results. Adhesive fracture energy is calculated from the formulae of British standards. The value of m is the gradient which is denoted as the length and the height of specimen. As m becomes greater at static experimental result, the maximum load becomes higher and the displacement becomes lower. And the critical fracture energy becomes higher. As m becomes less at fatigue experimental result, the displacement becomes higher and the critical fracture energy becomes higher. Fracture behavior of adhesive can be analyzed by this study and these experimental results can be applied into real field effectively. The stability on TDCB structure bonded with aluminum foam composite can be predicted by use of this experimental result. Adhesive fracture energy is calculated from the formulae of British standards. Based on correlations obtained in this study, the fracture behavior of bonded material would possibly be analyzed and aluminum foam material bonded with adhesive would be applied to a composite structure in various fields, thereby analyzing the mechanical and fracture characteristic of the material.

Keywords: Aluminum foam, Tapered double cantilever beam (TDCB), Fracture behavior, Adhesively bonded structures, Adhesive fracture energy

1. Introduction

Amid the growing industry, the metallic material has been widely used with the diversified material. Only a single material can be hardly satisfied in rigidity, corrosion resistance, abrasion resistance, lightweight, heat resistance and sound insulation performance. Hence, composite material is developed by combining or forming a number of singular materials to satisfy these requirements[1]. The composite material is also applicable to the structure with superior mechanical characteristic as functional material. The structural application is used at power generation, turbine engine, aerospace and industrial processing with high toughness, strength and heat resistance. The application as functional composite material is also used at electromagnetic component, sensors with electric and magnetic characteristics, medical applications with antibiotic performance and environmental material such as gas filter and catalytic converter with chemical performance. As described above, composite material is applied at various fields[2-5]. The fundamental study on fracture toughness data on glued joints to ensure safety in bonded structures is valuable. Recently, an evaluation method applying fracture mechanics for the strength evaluation of glued joints has been increasingly used. In case of the cracks propagated at opening mode(mode

I), TDCB specimen with inclined configuration has been used to identify the segregation among layers of composite material and evaluate fracture characteristic of adhesive interface, while the measurement method has been developed as standardized method for a long time[6-7]. In this study, the composite specimen of aluminum foam with mode I test is conducted in accordance with British standards BS 7991[8] and ISO 11343[9]. Adhesive fracture energy is calculated from the formulae of British standards. Based on the correlation obtained from this study, the analysis of fracture behavior is carried out and aluminum foam bonded by using adhesive is applied to the actual composite structure to analyze mechanical characteristic and fracture property[10-15].

2. Specimen

2.1. Configuration and dimension of specimen

The properties of aluminum foam are indicated in TABLE 1. Spray 77 manufactured by 3M is used to bond materials. The adhesive agent has the adhesive strength of 0.4MPa as spray type. Its major components are added to isohexane, cyclohexane and SBR Latex Polymer. As the method bond-

* DIVISION OF MECHANICAL & AUTOMOTIVE ENGINEERING, KONGJU NATIONAL UNIVERSITY, CHEONAN-SI, REPUBLIC OF KOREA

[‡] Corresponding author: jucho@kongju.ac.kr

ing two specimens, adhesive agent is spread on the adhesive surface first and 1 hour later once again. And then two specimens are bonded each other. The thickness of adhesive agent between two specimens becomes 0.3 to 0.4 mm as compressed state. More than 24 hours later at room temperature after bonding, the fatigue experiment is carried out. Fig. 1 shows the specimen and the dimension is indicated as mm. Four kinds of specimens are comprised of m values of 2, 2.5, 3, and 3.5 m is referred to the gradient of specimen which is expressed with the function of crack length(a) and specimen height(h). These specimens are manufactured by Foam Tech. company at Korea.

TABLE 1

Property of aluminum foam

Property	Value
Young's modulus(GPa)	2.374
Poisson's ratio	0.29
Density(kg/m ³)	400
Yield strength(MPa)	1.8
Shear strength(MPa)	0.92

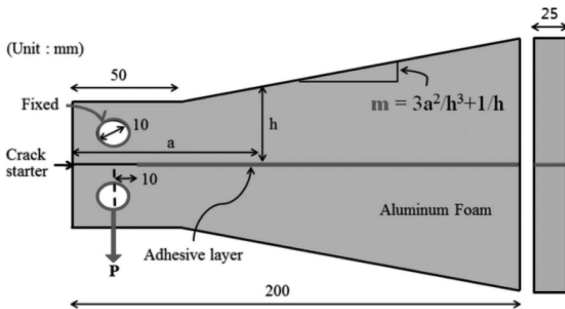


Fig. 1. Drawing of specimen

160N of repeated load downward while the cycle of loading is set to 2 cycles/s.

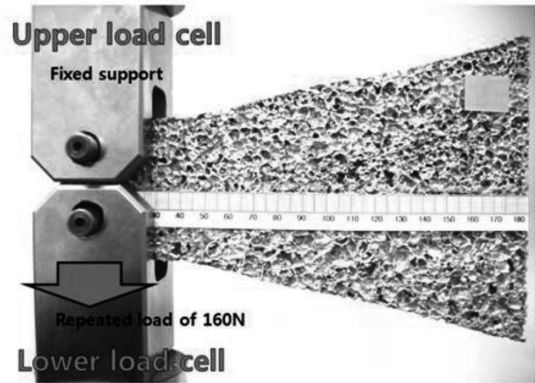


Fig. 3. Experimental setup at fatigue experiment

Fig. 4 shows the specimen with the tape indicating the number of divisions to measure the length of the crack. For more accurate test data, a number of specimens per case are produced to obtain the mean value statistically. Fig. 5 indicates the dimension of the specimens depending on the m value. As m value of specimen becomes larger, the slope becomes steeper.

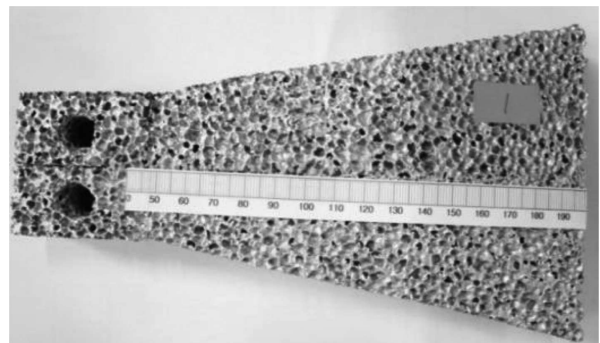


Fig. 4. Experimental specimen

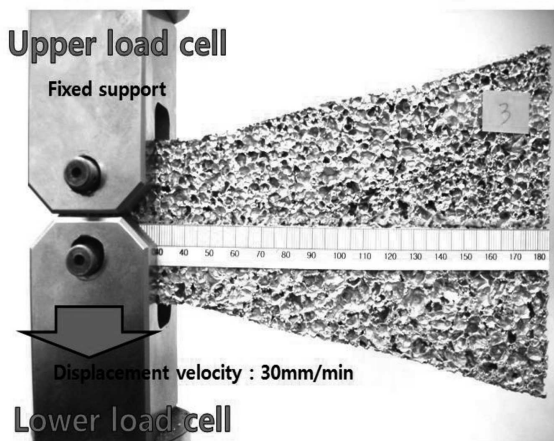


Fig. 2. Experimental setup at static experiment

As shown by Fig. 2, the specimen is fixed to the jig connected to the load cell of tester before conducting the static experiment by using displacement controlled method. Load is imposed downward on load cell for displacement and the displacement rate is set to 30 mm/min. The specimen is fixed to a jig connected to a load cell as seen by the fatigue experiment in Fig. 3. The fatigue experiment is carried out by imposing

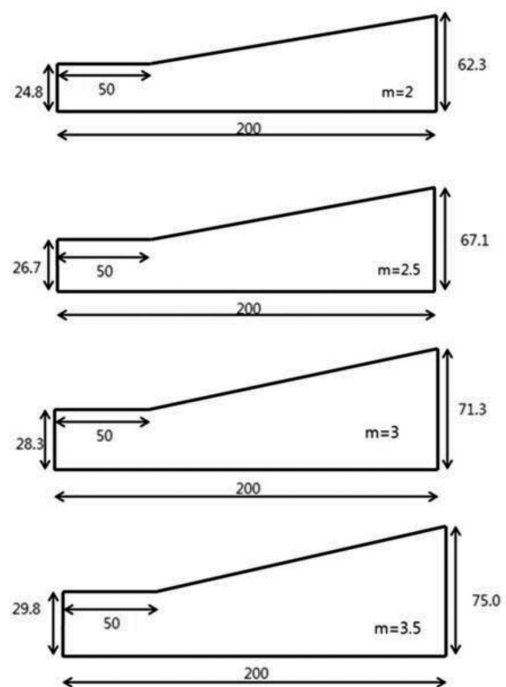


Fig. 5. Dimension of each specimen

2.2. Theory of fracture energy

B refers to the width of specimen and P is applied load. Form factor of specimen m is constant while the height of specimen varies according to the shape, which leads to Eq. 1[8].

$$\frac{3a^2}{h^3} + \frac{1}{h} = m \quad (1)$$

Crack length is and h refers to the thickness of beam on the crack tip of a vertical line. E_s refers to the modulus of elasticity of a bonding surface; thus, the fracture energy (G_{IC}) is calculated as indicated in Eq. 2 using Eq. 1.

$$G_{IC} = \frac{4P^2}{E_s B^2} \left(\frac{3a^2}{h^3} + \frac{1}{h} \right) = \frac{4P^2}{E_s B^2} \cdot m \quad (2)$$

However, in the existing SBT analysis, the compliance value of a specimen is calculated simply and accurately in general but no rotation or refraction on a crack tip is assumed to have existed. CBT analysis, however, considers the possible rotation on a crack tip. As the form factor of specimen, m is irrespective of $1/h$ of revision to shearing.

Thus the fracture energy (G_{IC}) under the load condition of mode I is calculated as Eq. 3.

$$G_{IC} = \frac{4P^2 m}{E_s B^2} \left[1 + 0.43 \left(\frac{3}{ma} \right)^{\frac{1}{3}} \right] \quad (3)$$

3. Experimental results

Fig. 6 is the graph showing the variation of G_{IC} which is the fracture energy at static experiment.

As the experimental static result, two curves on fracture energy due to crack length coincide from the beginning to 60 mm in cases of $m = 2$ and 2.5. As two specimens in these cases have slower slopes by comparing with others, these energies have the lowest values. The bending moment happens during de-bonding. During fracture, fracture energy depends on the configuration of specimen. As the slope becomes steeper, the value of m becomes greater and the bending moment becomes higher. As the bending moment becomes higher, the fracture energy becomes higher. As crack length becomes more than 170 mm, the fracture energies of G_{IC} values in cases of $m = 2, 2.5, 3$ and 3.5 converge each other as 180 J/mm². This means that the final fracture energy becomes constant regardless of m value at static experiment. The greater the value of m , the higher G_{IC} value, which keeps increasing up to the crack length from 1 to 150 mm and then begins to decrease or remains balanced which is attributable to the specimen which has been separated almost completely. Fracture energy increases gradually with similar gradient as crack increases.

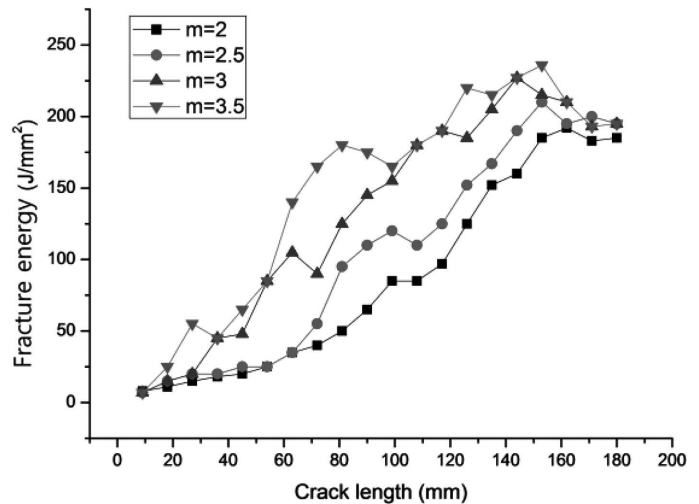


Fig. 6. Graph of fracture energy due to crack length (static experiment)

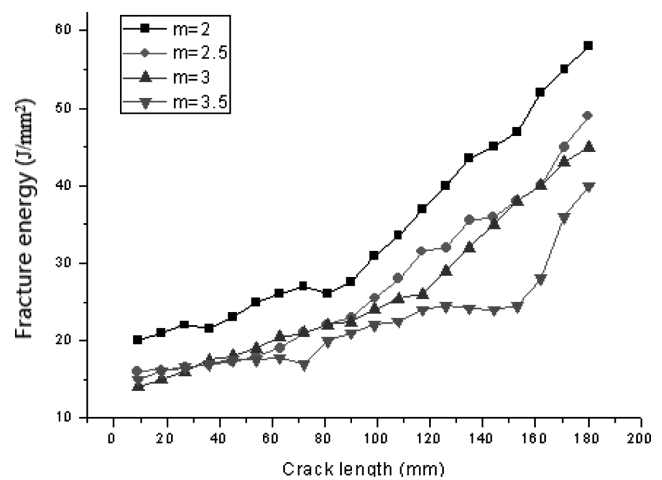


Fig. 7. Graph of fracture energy due to crack length (fatigue experiment)

Fig. 7 compares the fracture energy depending on the crack length of the specimen in the fatigue experiment.

As the experimental fatigue result, three curves on fracture energy due to crack length coincide nearly from the beginning to 60 mm in cases of $m = 2, 2.5$ and 3. As three specimens in these cases have steeper slopes, these energies have the lowest values. The bending force happens during de-bonding. Throughout fatigue fracture, fracture energy depends on the configuration of specimen. As the slope becomes slower, the value of m becomes smaller and the bending moment becomes higher. As the bending moment becomes higher, the fracture energy becomes higher. Fracture energy due to crack length in case of $m = 2$ with the slowest slope becomes highest among the cases of $m = 2, 2.5, 3$ and 3.5. And fracture energy due to crack length approach each other in cases of $m = 2.5$ and 3 during de-bonding. The fracture energy tends to increase in general while crack is developing. The fracture energy of the specimen with $m = 2$ appears to be the greatest, indicating 58 J/mm². The lower the value of m , the higher the fracture energy, which is due to a greater effect of the load and the displacement of fracture energy. These experimental results can be applied into real field effectively. The stability on TDCB structure bonded with aluminum foam

composite can be predicted by use of this experimental result. Adhesive fracture energy is calculated from the formulae of British standards. Based on correlations obtained in this study, the fracture behavior of bonded material would possibly be analyzed and aluminum foam material bonded with adhesive would be applied to a composite structure in various fields, thereby analyzing the mechanical and fracture characteristic of the material.

4. Conclusions

As a study result on the fracture experiment of TDCB specimen with bonded aluminum foam composite material, the following conclusion is summarized;

The bending moment happens during de-bonding. During fracture, fracture energy depends on the configuration of specimen. As the slope becomes steeper at the experimental static result, the value of m becomes greater and the bending moment becomes higher. As the bending moment becomes higher, the fracture energy becomes higher. As crack length becomes more than 170 mm, the fracture energies of G_{IC} values in cases of $m = 2, 2.5, 3$ and 3.5 converge each other as 180 J/mm^2 . The final fracture energy becomes constant regardless of m value at static experiment. Throughout fatigue fracture, fracture energy depends on the configuration of specimen. As the slope becomes slower, the value of m becomes smaller and the bending moment becomes higher. As the bending moment becomes higher, the fracture energy becomes higher. Fracture energy due to crack length in case of $m = 2$ with the slowest slope becomes highest among the cases of $m = 2, 2.5, 3$ and 3.5 . The lower the value of m , the higher the fracture energy, which is due to a greater effect of the load and the displacement of fracture energy. These experimental results can be applied into real field effectively. The stability on TDCB structure bonded with aluminum foam composite can be predicted by use of this experimental result. Adhesive fracture energy is calculated from the formulae of British standards. Based on correlations obtained in this study, the fracture behavior of bonded material would possibly be analyzed and aluminum foam material bonded with adhesive would be applied to a composite structure in various fields, thereby analyzing the mechanical and fracture characteristic of the material.

Acknowledgements

This research is supported by the Basic Science Research Program through the National Research Foundation of Korea (NRF) funded by the Ministry of Education, Science, and Technology (2011-0006548).

REFERENCES

- [1] A. Paul, U. Ramamurty, *Materials Science and Engineering: A* **281**, 1-2, 1-7 (2000).
- [2] J.U. Cho, A. Kinloch, B. Blackman, S. Rodriguez, C.D. Cho, S.K. Lee, *International Journal of Precision Engineering and Manufacturing* **11**, 1, 89-95 (2010).
- [3] N.Y. Chung, S.I. Park, *International Journal of Automotive Technology* **5**, 4, 303-309 (2004).
- [4] M. Todo, P.Y.B. Jar, *Composites Science and Technology* **58**, 1, 105-118 (1998).
- [5] Y.B. Park, M.H. Lee, H.Y. Kim, S.I. Oh, *International Journal of Automotive Technology* **6**, 6, 657-663 (2005).
- [6] P. Qiao, J. Wang, J.F. Davalos, *Engineering Fracture Mechanics* **70**, 2, 339-353 (2003).
- [7] A. Pirondi, G. Nicoletto, *Engineering Fracture Mechanics* **71**, 859-871 (2004).
- [8] Determination of the Mode I Adhesive Fracture Energy G_{IC} of Structure Adhesives Using the Double Cantilever Beam (DBC) and Tapered Double Cantilever Beam (TDCB) Specimens, British Standard, BS 7991 (2001).
- [9] International Standards Organization, ISO 11343, Geneva 1993.
- [10] A. Biel, U. Stigh, *Engineering Fracture Mechanics* **75**, 10, 2368-2983 (2008).
- [11] S.S. Kim, Study on Mechanical behavior of the Crack at Tapered Double Cantilever Beam with Aluminum Foam. Master Thesis, Kongju University, Cheonan Daero 1223-24, February.
- [12] S.S. Kim, M.S. Han, J.U. Cho, C.D. Cho, *International Journal of Precision Engineering and Manufacturing* **14**, 10, 1791-1795 (2013).
- [13] R. Ahmad, J.H. Ha, Y.D. Hahn, I.H. Song, *Journal of the Korean Powder Metallurgy Institute* **19**, 4, 278-284 (2012).
- [14] S.H. Lee, D.M. Hong, *Journal of the Korean Powder Metallurgy Institute* **21**, 1, 50-54 (2014).
- [15] J.H. Choi, S.S. Yang, Y.D. Kim, J.Y. Yun, *Journal of the Korean Powder Metallurgy Institute* **20**, 6, 439-444 (2013).